CHAPTER 5

Synthesis and Characterization of Coated Alumina Borate Whiskers

In this chapter, the procurement of research-related materials, experimental set-up, and the procedure for coating alumina borate with metal oxide is uniform. It doesn't alter the chemical composition of the composite. The present chapter is aimed to compare the effect of various coatings on the thermo-mechanical properties of alumina borate. Oxidation at high temperatures is a major challenge faced by ceramic coatings. However, they provide lubricity and sturdiness to ceramic. Ceramic coatings are often used in the automotive and aluminium industry as barrier materials to enhance the interaction between moving metal parts [98-105]. Four coatings were studied (Cr_2O_3, SiO_2, ZnO, and TiO_2) to make a comparative study of different metal oxides. The alumina borate (ABO) was made using the hydrolization route to prevent combustion and coating by the sol-gel method. To confirm the microstructural properties after coating was done by scanning electron microscopy (SEM) and energy dispersive spectroscopy (EDS) analysis. X-ray diffraction analysis (XRD) was performed for phase identification at different temperatures. The physical thermo-mechanical properties, i.e. bulk density, apparent porosity, and high-temperature modulus of rupture, were measured for different coated samples. The comparative study of the fabricated sample was presented at different parameters. Resultantly it was observed that the SiO_2 coated sample shows remarkable improved properties compared to other coated pieces. The strength achieved encourages the use of these materials for structural applications, especially due to their relatively low density and high porosity [106].

5.1. Morphological study of coated whiskers

5.1.1 HRSEM analysis of coated composites

The HRSEM micrographs of each sample of ABO powder with various coatings calcined at 1100 °C are shown in **Figure 5.1**. **Figure 5.1(a)** shows the Cr_2O_3 coating has a uniform surface. The thermo-mechanical properties increased as compared to ZnO coating because ZnO coating offers an uneven surface that degrades the mechanical properties. It can be seen in **Figure 5.1(b)** while the SiO_2 coating is smooth and compact and leaves no cavity and holes.

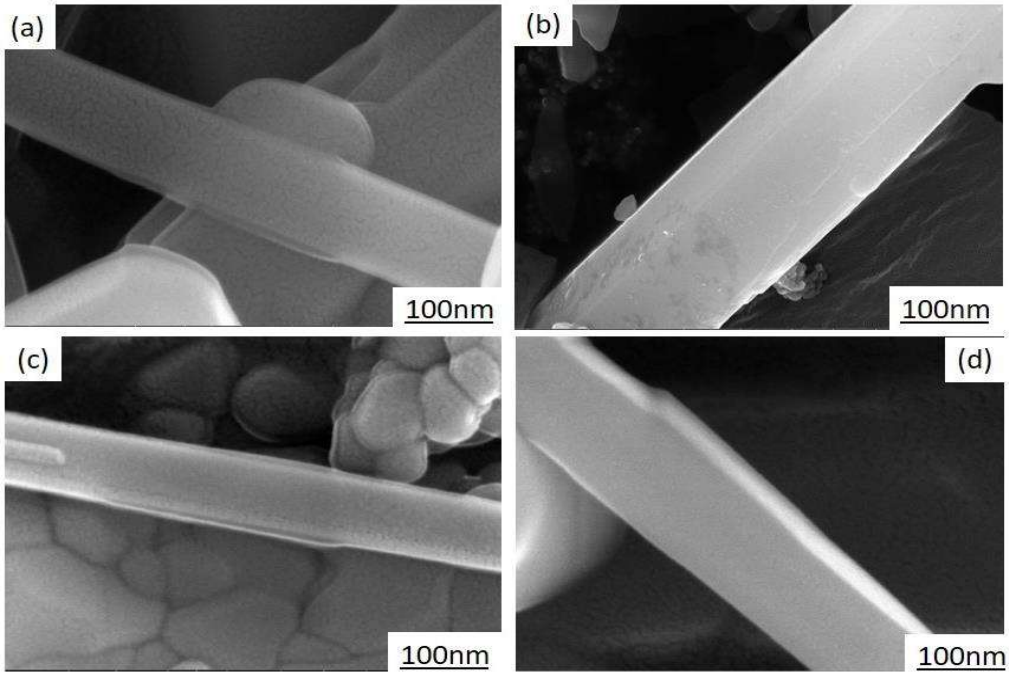

Figure 5.1: HRSEM image of ABO_w powder coated with **(a)** Cr_2O_3 **(b)** SiO_2 **(c)** ZnO **(d)** TiO_2

Figure 5.1(c) shows that the ZnO coating is coarser and has fluffy surfaces also, no significant improvement in mechanical properties was found. **Figure 5.1(d)** shows the TiO_2 coating, which exhibits uniform surface compared to SiO_2 coating and has excellent thermo-mechanical strength. Agglomerations are almost absent after coating

and calcining and coated layers of Cr_2O_3, SiO_2, ZnO, and TiO_2 film are observed to be uniformly distributed on the alumina borate whisker surface. The coating does not form an additive with base a compound due to the low percentage of the coating material. Apart from the comparative studies of different coating on ABO_w powder, the ABO_w powder sample matrix will significantly improve the thermo-mechanical properties with SiO_2 coatings. **Figure 5.2** shows the EDS point of each coating on ABO_w powder. The point indicates the presence of Al, B, O, and **Figure. 5.2 (a),** Cr in spot (1), **Figure 5.2 (b),** Si **Figure. 5.2 (c)** Zn and **Figure 5.2 (d)** Ti weight percentage in a specific region.

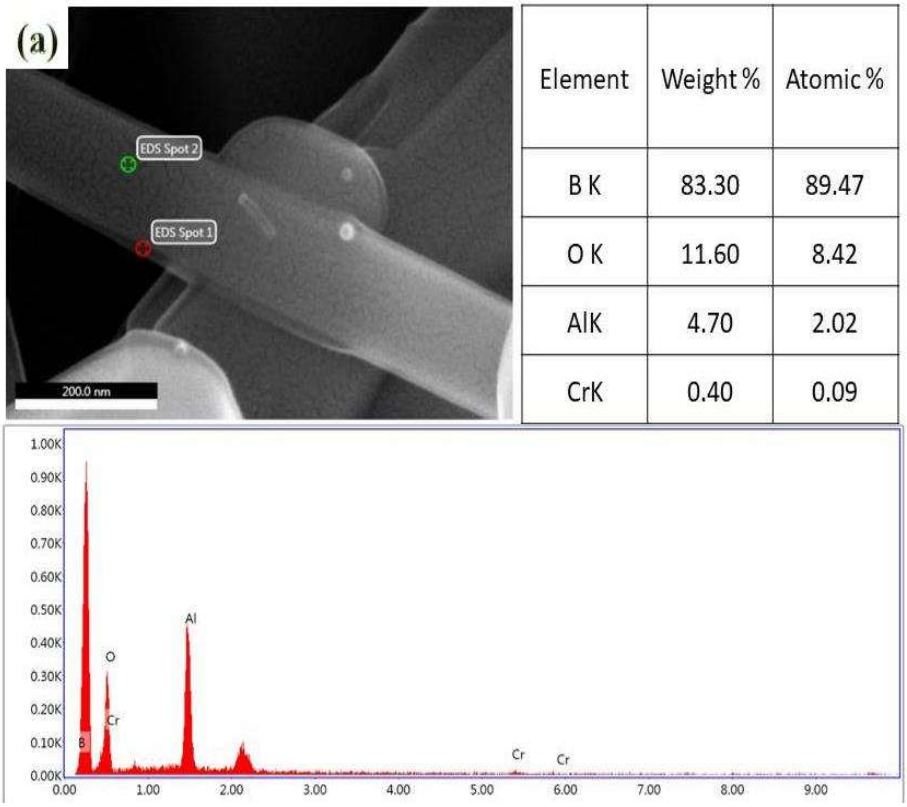

Element	Weight %	Atomic %
B K	83.30	89.47
O K	11.60	8.42
AlK	4.70	2.02
CrK	0.40	0.09

Figure 5.2:(a) The EDAX spectrum of Cr_2O_3 coated surface of ABO_w

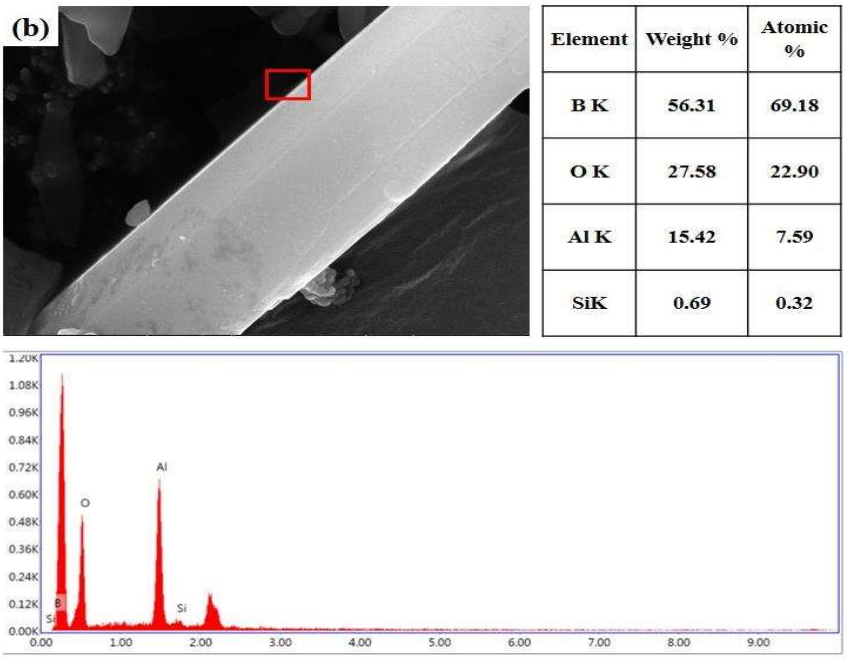

Element	Weight %	Atomic %
B K	56.31	69.18
O K	27.58	22.90
Al K	15.42	7.59
SiK	0.69	0.32

Figure 5.2:(b) The EDAX spectrum of SiO_2 coated surface of ABO_w

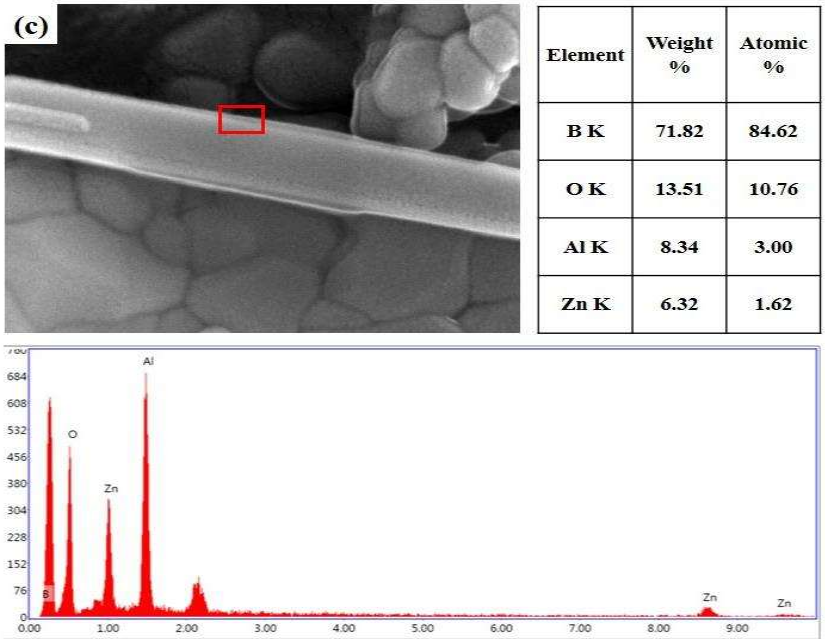

Element	Weight %	Atomic %
B K	71.82	84.62
O K	13.51	10.76
Al K	8.34	3.00
Zn K	6.32	1.62

Figure 5.2: (c) The EDAX spectrum of SiO_2 coated surface of ABO_w

No extra elements are present after the coating reaction, and each coated Nobel oxide has a uniform thin layer on the surface of ABO_w are formed.

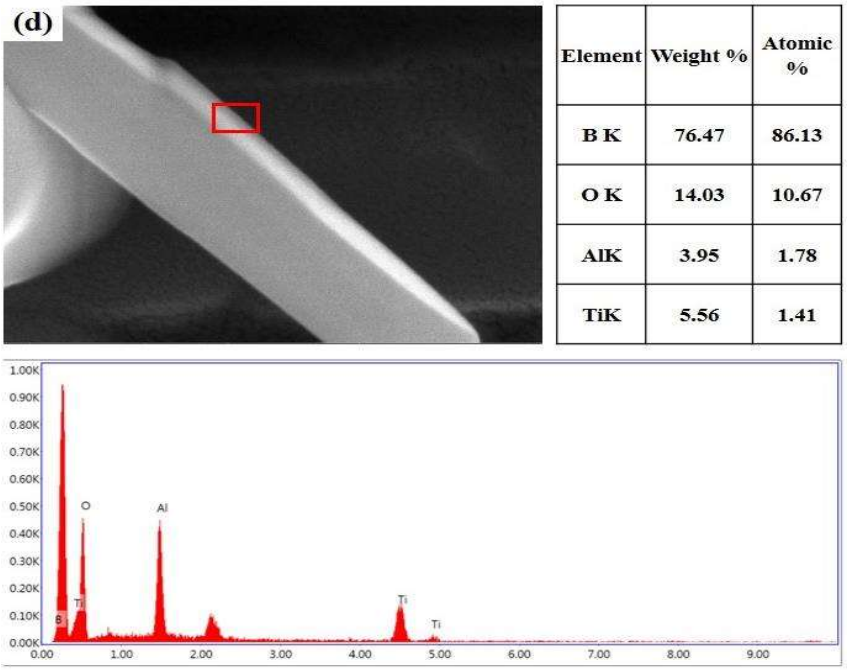

Element	Weight %	Atomic %
B K	76.47	86.13
O K	14.03	10.67
AlK	3.95	1.78
TiK	5.56	1.41

Figure 5.2:(d) The EDAX spectrum of TiO_2 coated surface of ABO_w

5.2 Phase evaluation of the coated samples

Figure 5.3 (a) & (b) shows X-ray diffraction (XRD) patterns of each metal oxide xerogel calcined at 500 °C for 4 h and 1100 °C temperatures for 1 h. It can be seen that the major phase was found of ABO ($Al_{18}B_4O_{33}$) (JCPDS-320003). ABO_w with Cr_2O_3 coating has Cr_2O_3 (JCPDS-841616) as the phase on both temperatures. ABO_w with the SiO_2 coating has beta quartz phase (JCPDS-750638) after increasing the calcining temperature to 500 °C, which changes to the tridymite phase (JCPDS-831832) at 1100 °C. This phase is uniformly found on the surface, and many peaks are formed at high temperatures. ABO_w with TiO_2 coating has a rutile phase (JCPDS- 760320) at both temperatures and ABO_w with ZnO coating has a white china phase (JCPDS-361451)

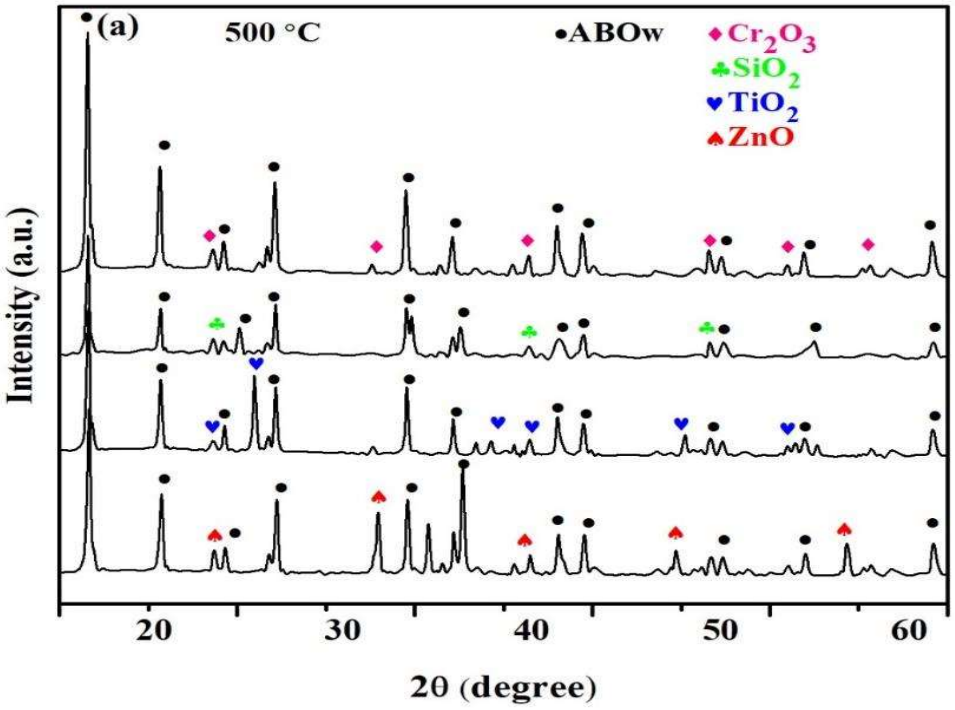

Figure 5.3: (a) XRD patterns of samples calcined at 500 °C for 4 h

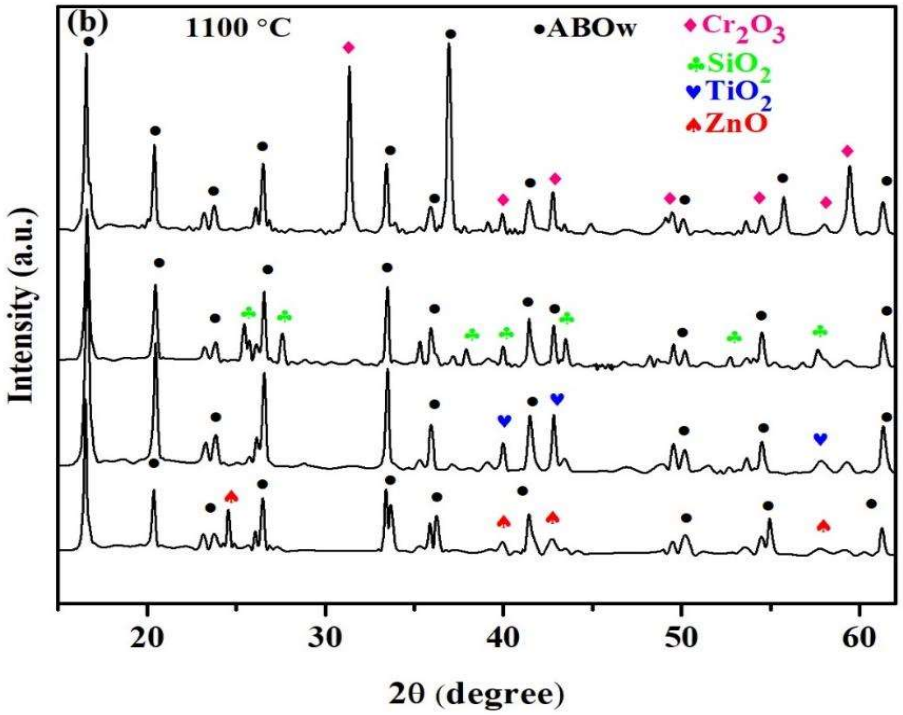

Figure 5.3: (b) XRD patterns of samples calcined at1100 °C for 1 h.

with hexagonal wurtzite structure at 500 °C, and ZnO has formed calcined at 1100 °C. The intensities of each coating diffraction peaks increase with increasing the calcining temperature, and no extra peaks were observed except Nobel oxide and ABO in each coating.

5.3 Water Absorption behaviour of the sintered sample

The water absorption behaviour viz. bulk density and apparent porosity of sintered samples are shown in **Table 5.1** and **Figure 5.4**. It is clear from a water absorption test, Cr_2O_3 has the lowest water absorption out of the four coatings and second in terms of bulk density, so this could also be resistant to acid attacks, thus proving its promising application in the chemical industry vessels [107]. In the case of SiO_2, with the density/porosity test and characterization, it is observed that with silica coating, the bulk density becomes highest, water absorption decreases, and apparent porosity becomes lowest. This might be because of the hydrophobic nature and tetrahedral structure of SiO_2 and the increase in the grain boundary of ABO_w [108].

Table 5.1 Physical (density/porosity) properties of uncoated and coated samples

S.No.	SAMPLE	BULK DENSITY	APPARENT POROSITY
1	ABOw	1.98	56.75
2	ABOw-Cr_2O_3	2.674	50.46
3	ABOw-SiO_2	3.377	32.57
4	ABOw-ZnO	2.44	59.82
5	ABOw-TiO_2	2.282	54.57

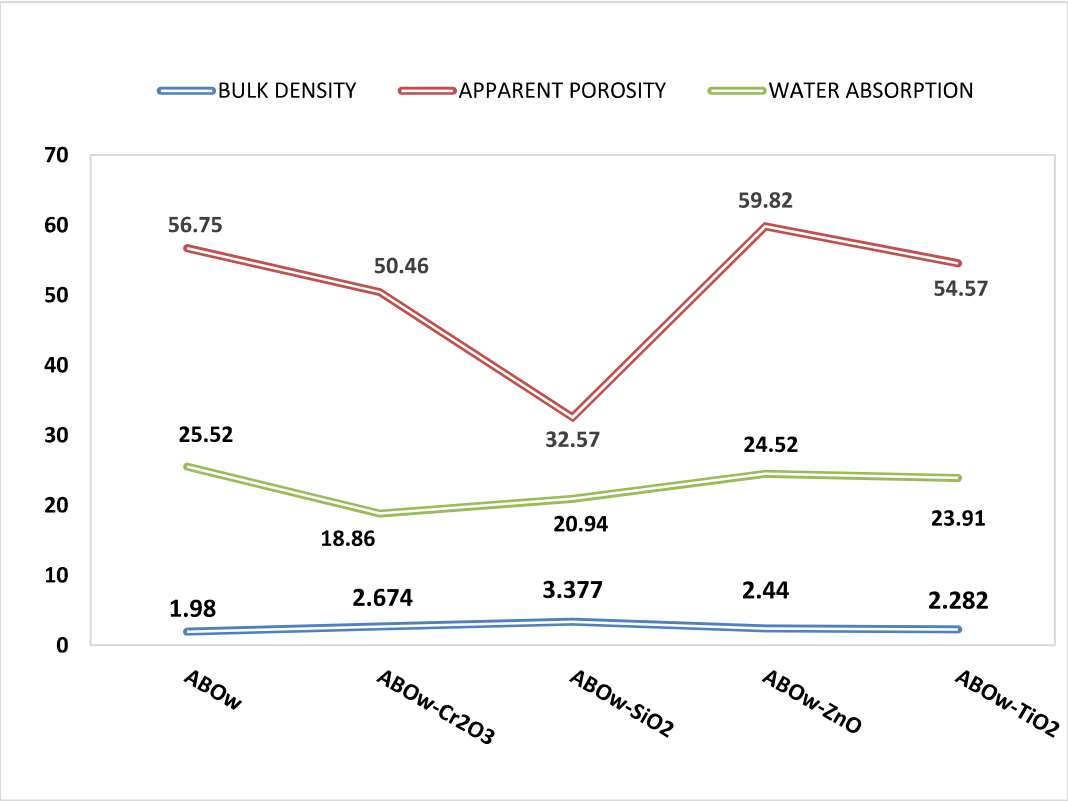

Figure 5.4: Physical properties (density/porosity) of coated samples

5.4. Thermo-Mechanical analysis of alumina boron refractories

Table 5.2 shows the MOR and HMOR properties of the coated and uncoated sintered ABO_w samples in the temperature range 27°C (room temperature), 800°C, and 1000°C. The maximum mechanical strength for the samples at room temperature was 65 ± 2.2 MPa and thermally treated at 800°C (53.1 ± 2.2 MPa). However it was decreased at 1000°C (51 ± 2.2 MPa) by adding the coated additive to the designed castables, the densification of SiO_2 coating was anticipated and the maximum HMOR values attained and were close to 800°C. This can be partly attributed to the greater bond between the ABO_w and coated layer as the curing time increases. Therefore, the composition of refractory castables can be a suitable option for applications that require enhanced

performance of the ceramic lining at intermediate temperatures (i.e., petro-chemical and aluminium production industries). Moreover, it was also observed that when increasing the testing temperatures (T > 800°C), the hot mechanical strength of the ZnO coated samples rapidly decreased due to agglomeration mainly after 1000°C. Moreover, for ABO_w samples, their strength decreases due to reactions that may include B_2O_3 volatilization at high temperatures; the high viscosity of borosilicate melts inhibits their crystallisation tendency.

Table 5.2 The HMOR properties of the coated and uncoated sintered samples

SAMPLE	27°C (MPa)	800°C (MPa)	1000°C (MPa)
ABOw	52±2.2	46±2.2	43±2.2
ABOw-Cr_2O_3	60±2.2	49±2.2	47±2.2
ABOw-SiO_2	65±2.2	53±2.2	51±2.2
ABOw-ZnO	52±2.2	46±2.2	43±2.2
ABOw-TiO_2	54±2.2	48±2.2	46±2.2

5.5 Fractograph of MOR sintered samples

Figure 5.5 (a), **(b), (c)** and **(d)** show the fractography of modulus of rupture (MOR) at 27°C of each coating. It can be observed that coated samples are not very much affected at room temperature, and no cracks were observed in the whiskers showing the high mechanical properties of the individual grains. SiO_2 coated whiskers

samples have uniform-grained microstructure and an optimum strength 65 ± 2.2MPa. Finally, the microstructures have a specific area and might be employed for heterogeneous catalysis and adsorption. However, the occurrence of clustering area and heavy irregularities in ZnO coated samples as shown in **Figure 5.5 (c)** indicates physical and chemical homogeneity within the samples.

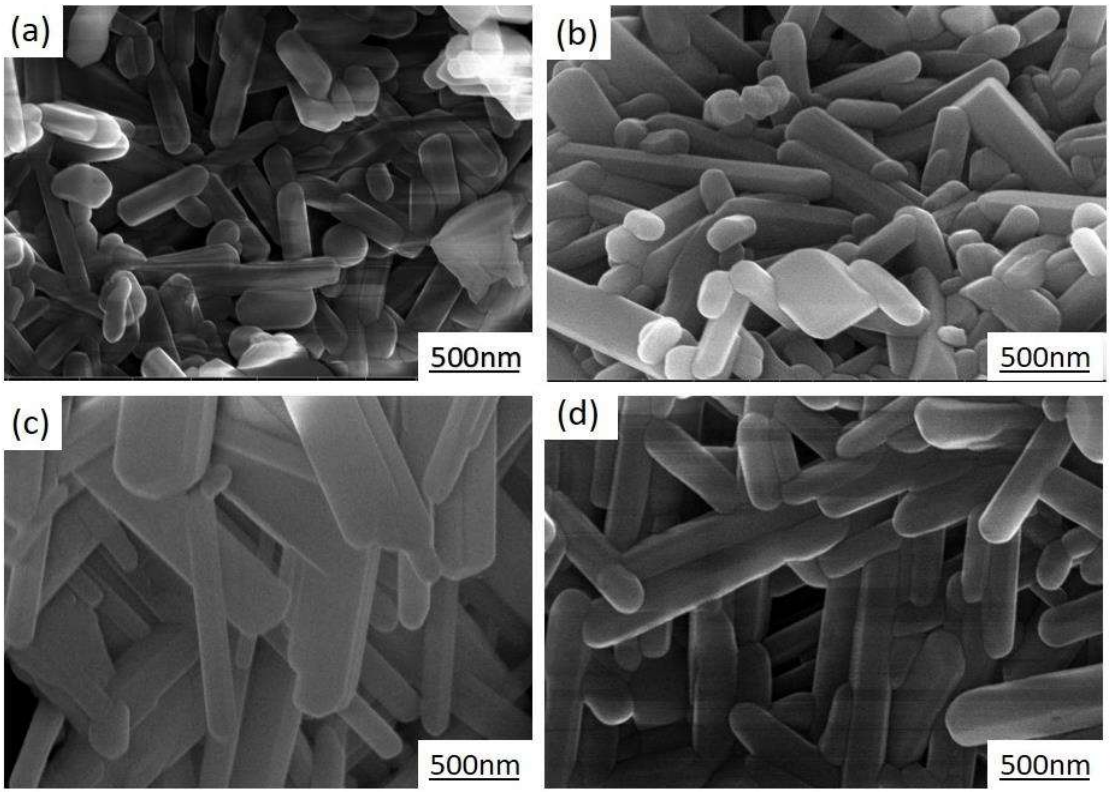

Figure 5.5: Fractogrpah of modulus of rupture at room temperature of **(a)** Cr_2O_3 **(b)** SiO_2 **(c)** ZnO **(d)** TiO_2 coated samples

This reaction might be degrading the mechanical property. Every mechanical property would be strongly affected by the microstructure and particularly by the porosity of the material, which, as described, is essential in these porous materials [109-110]. The porous structure and reasonable strength values make the material a potential candidate for ceramic filters and ceramic-metal composite preforms.

5.6 Fractograph of HMOR sintered samples

It can be observed that due to an increase in temperature and mechanical stress Cr_2O_3, SiO_2 and TiO_2 coated whiskers grow into feathery like structures and clustering occurs. Although, in the case of ZnO most of the whiskers are destroyed and agglomerated hence the flaky structure is observed as shown in **Figure 5.6 (d)**. The higher temperature treatments and morphology were gradually smoothed and different orientations under load and temperature.

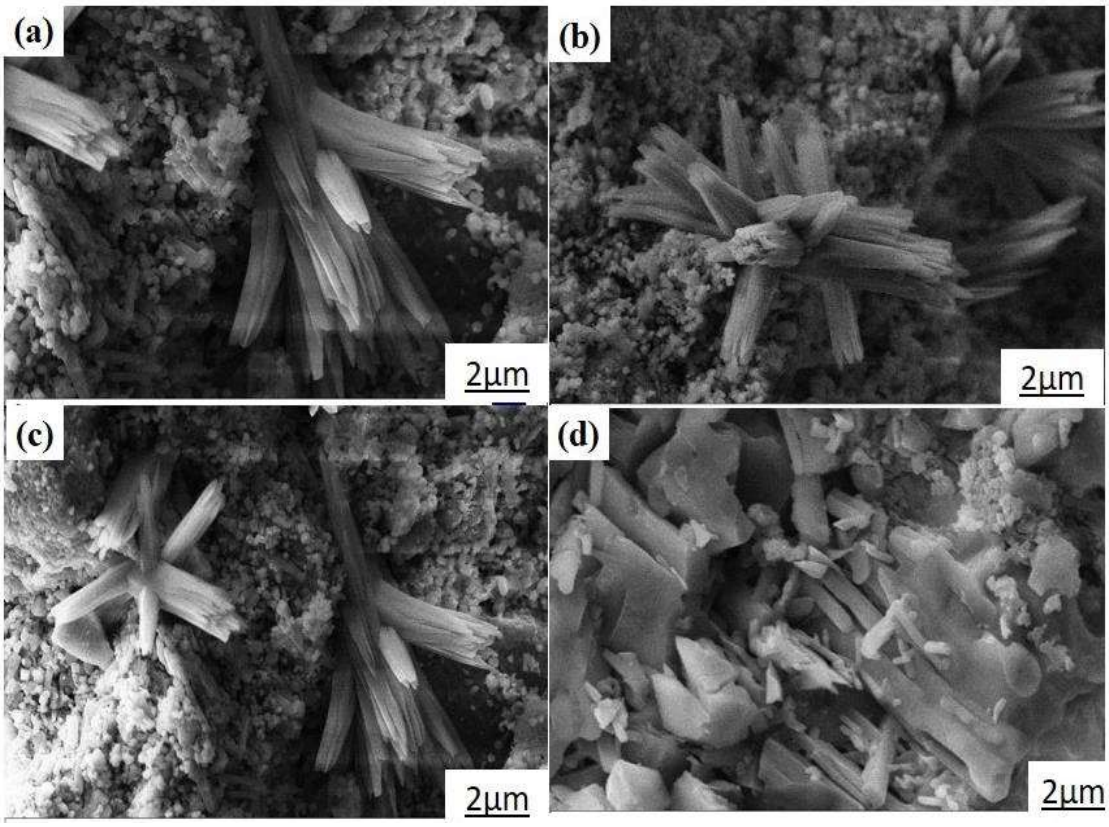

Figure 5.6: Fracture surface after the HMOR test at 1000 °C of **(a)** Cr_2O_3 **(b)** SiO_2 **(c)** ZnO **(d)** TiO_2 coated samples

The aspect ratio qualitatively decreased with increasing testing temperature. However, the thickness observed was in all the cases submicronic. On the other hand, HMOR at 1000°C is shown in **Figure 5.7** show quite a different structure from 800°C.

As shown in **Figure 5.7 (a), (b)**, and **(c)**, it was observed that when the test temperature was increased, more agglomeration occurred and feathery structure destroyed and structures became flaky and more voids are found due to more adhesion force.

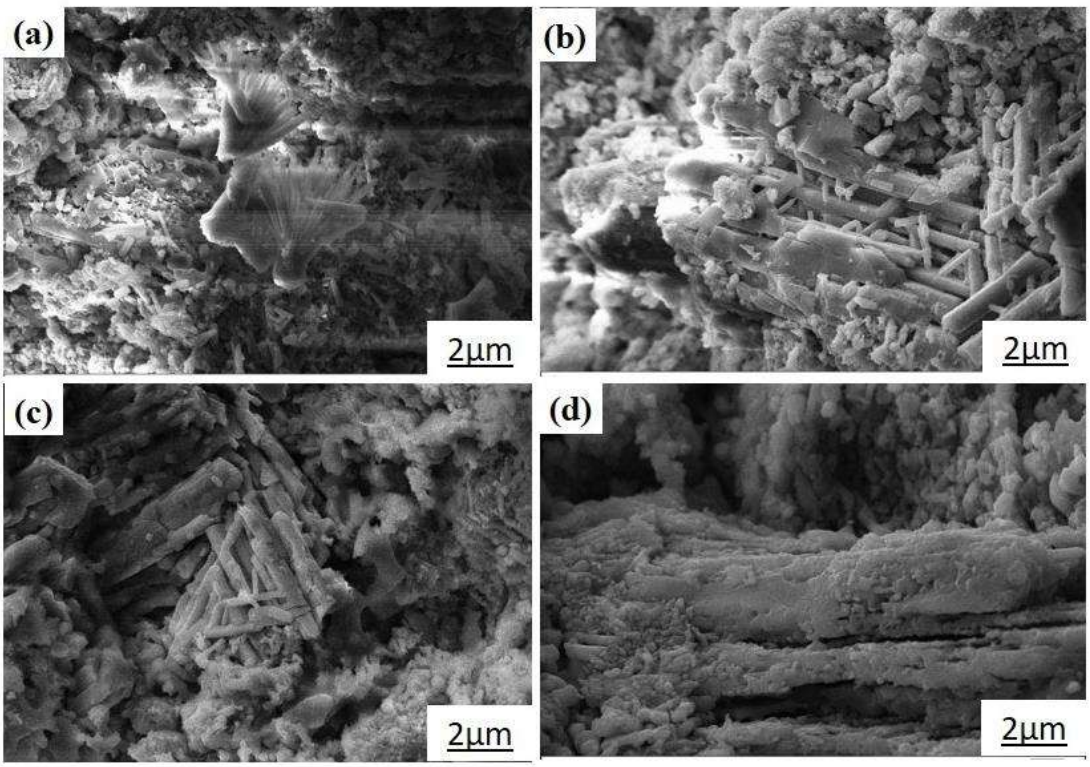

Figure 5.7: Fracture surface after the HMOR test at1000 °C room temperature of **(a)** Cr_2O_3**(b)** SiO_2 **(c)** ZnO**(d)** TiO_2 coated samples

It can be seen in **Figure 5.7(d)** due to vaporization at 1000°C as-grown colloidal spheres of ZnO create more voids which is the primary reason for degradation in the high-temperature modulus of rupture. Due to the partially heated and under the high stress, fracture behaviour presented high porosity (reaching 70%) interlocked (submicronic in diameter) needles, with no preferential orientation. Moreover, in the case of SiO_2 fracture image is not very much affected. This might be because of the hydrophobic nature and tetrahedral structure of silica and also the increase in the grain

boundary of ABO_w. SiO_2 coating thus formed on the surface of whiskers prevented viscous sintering and helped retain their aspect ratio at high temperatures. This might lead to better performance of such composites at higher temperatures [131].

5.7 Chapter summary

In this chapter, different coating on ABO_w powder samples has been carried out by the hydrolyzation process and based on results and discussion, it was analysed that the physical properties like density and porosity have been carried out and it was found that SiO_2 coating samples have higher density and lower apparent porosity and significantly improve the compactness of each coating by filling in the pores and cracks between each coated grain. The XRD images show the presence of different phases formed after coating the samples, and EDS confirm the presence of uniform coating. SiO_2 is strongest because of its high density and low porosity. Also, some % of beta quartz is formed at 500ºC, and 1100ºC tridymite is formed, which has very fine grain crystals. It also increases the strength and contact between the whiskers. In mechanical behavior the MOR and HMOR test analysis, amongst different coatings, SiO_2 coating samples show the higher thermo-mechanical strength at 27°C, 65 ± 2.2 MPa, 800ºC, 53 ± 2.2 MPa and 1000ºC, 51 ± 2.2 MPa. The order of thermo-mechanical strength values are $SiO_2 > Cr_2O_3 > TiO_2 > ZnO$. The SEM image of ZnO shows a lot of aggregation and cluster formation. It can also be observed that degradation in the HMOR properties compared to other coatings is due to high porosity. Cr_2O_3 also shows high strength because of the hexagonal crystal structure and compact packing. The fracture surface after the HMOR test found out that most of the whiskers have feathery-like structures at 800ºC. However, after increasing the test temperature to 1000ºC most of the fractography shows flaky structure due to more adhesion force and heating temperature.